THE JOURNAL OF PHYSICAL CHEMISTRY LETTERS
A JOURNAL OF THE AMERICAN CHEMICAL SOCIETY

pubs.acs.org/JPCL

Letter

Remarkable Insensitivity of Protein Diffusion to Protein Charge

Setare Mostajabi Sarhangi and Dmitry V. Matyushov*

Cite This: J. Phys. Chem. Lett. 2024, 15, 9502−9508

Read Online

ACCESS | Metrics & More | Article Recommendations | Supporting Information

ABSTRACT: Friction to translational diffusion of ionic particles in polar liquids should scale linearly with the squared ion charge, according to standard theories. Substantial slowing of translational diffusion is expected for proteins in water. In contrast, our simulations of charge mutants of green fluorescent proteins in water show remarkable insensitivity of the translational diffusion constant to protein's charge in the range of charges between −29 and +35. The friction coefficient is given as a product of the force variance and the memory function relaxation time. We find remarkably accurate equality between the variance of the electrostatic force and the negative cross-correlation of the electrostatic and van der Waals forces. The charge invariance of the diffusion constant is a combined effect of the force variance and relaxation time invariances with the protein charge. The temperature dependence of the protein diffusion constant is highly non-Arrhenius, with a fragile-to-strong crossover at the glass transition.

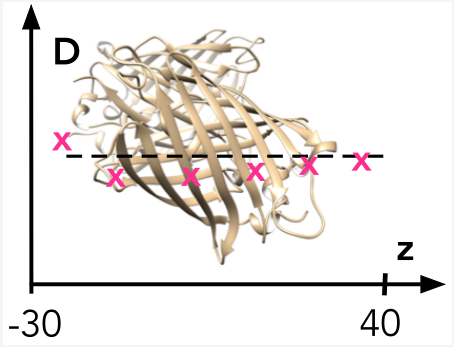

Friction produced by the medium on the diffusing particle is the main factor that determines the diffusion constant D through the Einstein equation

$$D^{-1} = \beta\zeta \tag{1}$$

Here, ζ is the friction coefficient and $\beta = (k_B T)^{-1}$ is the inverse temperature. Following the original hypothesis of Einstein,[1] hydrodynamic friction has been applied to diffusion of colloidal (Brownian) particles and even to individual molecules in the form of the Stokes−Einstein equation connecting ζ to liquid's shear viscosity η and the particle's radius R: $\zeta = \zeta_H = 6\pi\eta R$. Born suggested[2] that the Stokes−Einstein description of friction is incomplete for multipoles diffusing in polar liquids, where friction due to electrostatic forces (dielectric friction) has to be included. Theories of dielectric friction that followed[3−5] were based on Born's additivity assumption, allowing one to add the dielectric friction coefficient ζ_D to the hydrodynamic component:[6] $\zeta = \zeta_H + \zeta_D$. The result of this assumption is the prediction of the inverse diffusion constant to scale linearly with the squared ionic charge q for translational diffusion of ions.[4] Likewise, the inverse rotational diffusion constant is predicted[3] to scale linearly with the squared dipole moment M

$$D^{-1} = D_0^{-1} + aq^2\langle(\delta E)^2\rangle\tau_E,$$
$$D_r^{-1} = D_{0r}^{-1} + bM^2\langle(\delta E)^2\rangle\tau_E \tag{2}$$

Here, $D_0 = (\beta\zeta_H)^{-1}$ and D_{0r} refer to hydrodynamic translational and rotational diffusion constants, respectively. The numerical coefficients a, b are specified by analytical theories or numerical simulations. Included in the above scaling is the product of the relaxation time τ_E and the variance $\langle(\delta E)^2\rangle$ of the electric field of medium $\mathbf{E}$ acting on the diffusing multipole. The product qE in the first equation is the magnitude of the electric force acting on the moving ion. The dipole moment M in the second equation affects the rotational diffusion constant through the fluctuating torque $M\delta E \sin\theta$ connecting it to the electric field fluctuation δE, where θ is the angle between $\mathbf{M}$ and $\delta\mathbf{E}$. A statistical average over angles θ introduces a constant parameter absorbed in proportionality constant b in eq 2.

The anticipated scaling of the translational and rotational diffusion constants with the corresponding solute multipoles approximately holds for small ionic and dipolar solutes in water when tested by molecular dynamics (MD) simulations, even though the additivity assumption is consistently violated.[7,8] However, the standard theory seems to fail dramatically when applied to the translational diffusion of proteins in water. First, the relaxation time τ_E is significantly longer for solvated proteins than for small electrolyte ions and dipolar solutes. Combined with a large variance of the electric field due to elastic deformations of the protein surface carrying ionized surface residues, the standard equations produce large friction coefficients inconsistent with the reported diffusion constants for proteins in water.[8] In addition, and in stark contrast to the predictions of standard theories, a set of previous simulations of azurin mutants in water[9] with q changing from $q = 0$ to $q =$

Received: July 13, 2024
Revised: August 27, 2024
Accepted: September 6, 2024

https://doi.org/10.1021/acs.jpclett.4c02062
J. Phys. Chem. Lett. 2024, 15, 9502−9508

$-5e$ produced D insensitive to q, implying no significant dielectric friction. The theory-simulation contradiction was explained by the breakdown of the Born's additivity assumption and strong cross-correlations between fluctuations of osmotic (van der Waals, vdW) and electrostatic (E) forces kicking proteins into diffusive motion. Friction from electrostatics cannot, therefore, be separated from friction produced by density fluctuations modulating vdW forces. The purpose of this study is to show that strong E-vdW correlations are not limited to a single set of protein mutants, to further explore the molecular details of these cross correlations, and to clarify reasons for the failure of standard theories of molecular friction.

Here, we substantially extend the range of protein charges by taking advantage of an exceptional stability of green fluorescence proteins (GFPs) to charge mutations.[10−13] The charge range to study protein diffusion is strongly broadened to $-29 \le z \le 35$, $q = ez$ (see the Supporting Information, SI). We find a remarkable lack of sensitivity of D to changes in the protein charge, even in this largely extended charge range. We confirm the stability of the compensation relation between the vdW-E cross-correlation and the electric force variance found in previous simulations.[7,9] We additionally study for the first time the stability of this relation to temperature changes by simulations of another globular protein, plastocyanin (PC) in the range of temperatures 100−400 K in TIP3P water.[14] Remarkably, the compensation relation remains stable in the entire temperature range, despite reported structural crossovers of the protein hydration shell around the temperature of dynamical transition.[15−18] All protein simulations were performed without electrolyte ions to avoid complications from the electrolyte friction. The uniform background charge arising from applying Ewald sums with the overall charged simulation box[19] does not affect our results because only the field fluctuation $\delta\mathbf{E}$ enters our calculations.

The temperature dependence of the diffusion constant for PC is found to be strongly non-Arrhenius, with signatures of the strong-to-fragile crossover[20] near the glass transition of hydration water at $T_{tr} \simeq 170$ K.[15] This feature is related to protein−water electrostatics, as the variance of the electrostatic force acting from hydration water on the protein passes through a sharp peak at $T \simeq 200$ K. An even stronger peak, at the same temperature, is found for the rotational relaxation time of the protein dipole.

The standard Stokes−Einstein framework does not provide a microscopic view of the physical forces promoting diffusion. Einstein viewed diffusion as driven by osmotic forces,[1] which, in the modern language, can be identified with the collective density fluctuations modifying vdW forces acting from the interfacial liquid on the tagged particle. In contrast to the Stokes−Einstein perspective, the Kirkwood equation allows one to treat the problem from the perspective of physical random forces acting on the diffusing particle. The starting point here is the memory equation[21] for the velocity-velocity autocorrelation function $C_v(t) = \langle \mathbf{v}(t)\cdot\mathbf{v}(0)\rangle$. The corresponding normalized correlation function, $\Phi_v(t) = C_v(t)/C_v(0)$, satisfies the memory equation[21,22]

$$\dot{\Phi}_v(t) + \int_0^t d\tau M_v(t-\tau)\Phi_v(\tau) = 0 \tag{3}$$

Here, the memory function $M_v(t)$ propagates short-range, local dynamics to more collective dynamics of $\Phi_v(t)$.[23] The memory function $M_v(t)$ can be factorized into its $t = 0$ value and a normalized time-dependent function $m(t)$

$$M_v(t) = M_v(0)m(t), \qquad M_v(0) = \frac{\langle \dot{\mathbf{v}}^2\rangle}{\langle \mathbf{v}^2\rangle} = \frac{\beta}{3M}\langle(\delta\mathbf{F})^2\rangle \tag{4}$$

where M is the mass of the diffusing particle. The Fourier−Laplace transform of eq 3 yield

$$\tilde{\Phi}_v(\omega) = [-i\omega + \tilde{M}_v(\omega)]^{-1} \tag{5}$$

where tildes denote the Fourier−Laplace transforms of the corresponding time dependent functions.

Equation 5 connects the diffusion constant,[21] $D = (\langle \mathbf{v}^2\rangle/3)\tilde{\Phi}_v(0)$, to the statistics and dynamics of random forces

$$D^{-1} = \frac{1}{3}\beta^2\langle(\delta\mathbf{F})^2\rangle\tau_m \tag{6}$$

The friction coefficient in the Einstein eq (eq 1) is thus the product of the force variance and the integral memory relaxation time

$$\tau_m = \tilde{m}(0) = \int_0^\infty \mathrm{d}t m(t) \tag{7}$$

Equation 6 is exact, while the Kirkwood equation is an approximation replacing τ_m with the force relaxation time τ_F, that is the area under the curve of the normalized force−force time correlation function

$$\tau_F = \int_0^\infty \mathrm{d}t \Phi_F(t) \tag{8}$$

where

$$\Phi_F(t) = \langle(\delta\mathbf{F})^2\rangle^{-1}\langle\delta\mathbf{F}(t)\cdot\delta\mathbf{F}(0)\rangle \tag{9}$$

One obtains $\tau_m \to \tau_F$ in eq 6, restoring the Kirkwood equation, when the solute is much heavier than the solvent.[8,24] Deviations from the exact formula can be derived as a series expansion in the square root of the ratio of the solvent, m_s, and solute, M, masses.[22] Recent molecular dynamics (MD) simulations have shown that this expansion starts with the second-order term and the first nonvanishing correction scales as m_s/M.[24] Based on this scaling, diffusion of proteins in water is expected to follow the Kirkwood equation. However, we find from our MD simulations that $\tau_m \simeq 2\tau_F$, while both of them maintain essential independence of the protein charge (Table 1).

Table 1. Relaxation Times of Component Forces and of the Total Force (ps)[a]

z	$\langle M\rangle$, D	τ_E	τ_{LJ}	τ_F	τ_m	τ_M	τ_r
−29	354	1.28	0.60	0.012	0.023	1871	1837
−15	413	1.09	0.50	0.013	0.025	14968	20121
−6	293	1.14	0.64	0.013	0.027	1104	1125
10	309	1.48	0.69	0.016	0.028	1740	1855
25	256	1.61	0.78	0.016	0.029	5288	5113
35	510	2.13	1.05	0.014	0.026	3475	3795

[a]Also shown are the integral memory time τ_m calculated from D and $\langle(\delta\mathbf{F})^2\rangle$ in eq 6 and the relaxation time of the protein dipole τ_M and the rotational relaxation time τ_r.

https://doi.org/10.1021/acs.jpclett.4c02062
J. Phys. Chem. Lett. 2024, 15, 9502−9508

The memory relaxation times τ_m in Table 1 were calculated from the force variance discussed below and the diffusion constant of proteins according to eq 6. The diffusion constants D are from MD simulations of protein mutants of GFP and PC in the temperature range of 100−400 K. The calculations use mean-squared displacements (MSD) $\langle \Delta r^2(t) \rangle$ according to the relation

$$D_{\mathrm{MD}} = (6t)^{-1} \langle \Delta r^2(t) \rangle \tag{10}$$

The diffusion constants from MD, D_{MD}, were corrected for the finite size of the simulation box according to the following equation[25]

$$D = D_{\mathrm{MD}} + 2.837297 k_{\mathrm{B}} T/(6\pi\eta L) \tag{11}$$

where L is the length of the simulation box and η is the solvent viscosity for which the value for TIP3P, η = 0.306 cP, was adopted.[26] Our diffusion constants (Table 2) are somewhat lower than ≃ 82−87 $\mu m^2/s$[27−30] reported for GFPs in water. Experimental diffusion constants are lower for eukaryotic cytoplasm, ≃ 27 $\mu m^2/s$.[31] A quantitative agreement between experimental and simulated diffusion constants is not anticipated with the existing force fields given that even the self-diffusion constant of bulk water is not reproduced by the TIP3P model (5.48×10^{-5} cm^2/s for TIP3P vs 2.30×10^{-5} cm^2/s for water[32]). The results for GFP mutants are compared to azurin mutants[9] in Figure 1a. We note that the ratio of diffusion coefficients for two sets of proteins is inconsistent with the ratio of the corresponding radii, which one would anticipate from the Stokes−Einstein law.

Table 2. D ($\mu m^2/s$) According to eqs 10 and 11 vs the Charge $q = ze$ of GFP Mutants

z	D_{MD}	D
−29	22.01	22.03
−15	23.65	23.67
−6	20.83	20.85
10	20.42	20.44
25	20.84	20.86
35	21.08	21.10

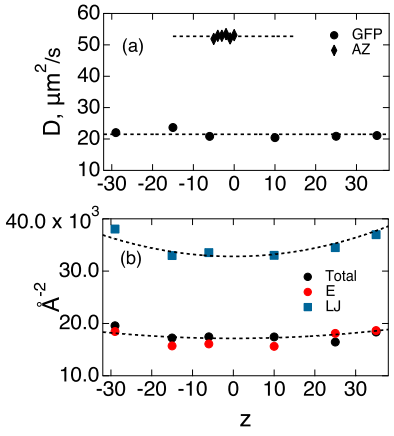

Figure 1. (a) Diffusion constants of GFP (circles) and azurin (AZ, diamonds) mutants[9] vs the protein charge $q = ez$. The ratio of average values (horizontal lines) is 2.45. The ratio of GFP and arurin radii is 1.34 (R(GFP) ≃ 19.3 Å, R(AZ) ≃ 14.4 Å,[9] see SI). (b) Components of the force variance $\beta^2\langle(\delta \mathbf{F})^2\rangle/3$ (Å^{-2}). The dashed lines show polynomial fits of the vdW component of the variance (32921.5 + 4.10376z^2, Å^{-2}) and of the total variance (17341.9 + 1.35959z^2, Å^{-2}).

We confirm here the finding for azurin of a compensation relation[8] between the vdW (Lennard-Jones, LJ) and electrostatic forces acting from water on the protein. This general result was confirmed for diffusion of gold nanoparticles[33] and even for self-diffusion of water.[34] Compensation arises from separating the total force $\mathbf{F} = \mathbf{F}_{\mathrm{E}} + \mathbf{F}_{\mathrm{LJ}}$ acting on the protein from water to the electric, $\mathbf{F}_{\mathrm{E}}$, and LJ, $\mathbf{F}_{\mathrm{LJ}}$, components. The force variance is then a sum of component variances and a cross term

$$\langle(\delta \mathbf{F})^2\rangle = \langle(\delta \mathbf{F}_{\mathrm{E}})^2\rangle + \langle(\delta \mathbf{F}_{\mathrm{LJ}})^2\rangle + 2\langle \delta \mathbf{F}_{\mathrm{E}} \cdot \mathbf{F}_{\mathrm{LJ}}\rangle \tag{12}$$

We found (Table 3) that the relation[8,9]

$$\langle(\delta \mathbf{F}_{\mathrm{E}})^2\rangle = -\langle \delta \mathbf{F}_{\mathrm{E}} \cdot \mathbf{F}_{\mathrm{LJ}}\rangle \tag{13}$$

Table 3. Variances of Electrostatic and LJ Force Components and Their Cross Term vs the Protein Charge[a]

z	E	LJ	E-LJ	total
−29	18461	38037	−18469	19560
−15	15699	32982	−15728	17226
−6	16091	33546	−16094	17449
10	15616	33027	−15609	17425
25	18105	34494	−18079	16440
35	18635	36975	−18630	18350

[a]All parameters are given as $\beta^2\langle(\delta \mathbf{F})^2\rangle/3$ (Å^{-2}) consistent with eq 6.

holds very accurately, thus yielding a compensatory relation between the component variances in the total force variance

$$\langle(\delta \mathbf{F})^2\rangle = \langle(\delta \mathbf{F}_{\mathrm{LJ}})^2\rangle - \langle(\delta \mathbf{F}_{\mathrm{E}})^2\rangle \tag{14}$$

While eq 14 holds very accurately, one also finds an approximate relation $\langle(\delta \mathbf{F})^2\rangle \simeq \langle(\delta \mathbf{F}_{\mathrm{E}})^2\rangle$ (Figure 1b), which, however, does not hold for azurin mutants.[9]

Equation 14 results in a cancellation of changes of component variances with the protein charge. Both $\langle(\delta \mathbf{F}_{\mathrm{LJ}})^2\rangle$ and $\langle(\delta \mathbf{F}_{\mathrm{E}})^2\rangle$ increase with the protein charge $q = ez$ and can be approximated by broad parabolas of z ($a + bz^2$, dashed lines in Figure 1b). However, there is much less variation of the total variance with z because of the compensation. The near independence of D of the protein charge is a combined effect of the constancy of the force variance (Table 3) and the constancy of τ_m and τ_{F} (Table 1).

Table 1 additionally lists the relaxation times of the component forces (LJ and E), along with the values of τ_{F} and τ_m. The reported relaxation times are integrals of the corresponding time correlation functions

$$\tau_a = \int_0^\infty \mathrm{d}t S_a(t) \tag{15}$$

where a = E, LJ, F (the fitting protocol for the correlation functions is explained in the SI). Relaxation of the electrostatic force is the slowest among the correlation functions considered (Figure 2), with relaxation of the total force occurring on a time scale about 2 orders of magnitude faster. The strong cross-correlation between E and LJ components seen for the force magnitudes also extends to the dynamics: the total force is always much faster than the component forces.

https://doi.org/10.1021/acs.jpclett.4c02062
J. Phys. Chem. Lett. 2024, 15, 9502−9508

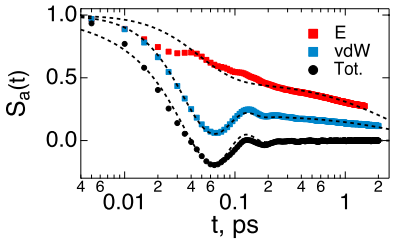

Figure 2. Normalized time autocorrelation functions $S_a(t)$, a = Tot, E, LJ of the total force and of the force components for GFP with $z = -6$. The dashed lines show fits to analytical functions (see SI).

Table 1 also reports two additional relaxation times related to the dynamics of the protein dipole moment: the dipole moment relaxation time τ_M and the rotational relaxation time τ_r. The former characterizes the normalized time correlation function of the protein dipole $\mathbf{M}(t)$

$$\Phi_M(t) = \langle (\delta M)^2 \rangle^{-1} \langle \delta\mathbf{M}(t)\cdot\delta\mathbf{M}(0)\rangle \tag{16}$$

where $\delta\mathbf{M}(t) = \mathbf{M}(t) - \langle\mathbf{M}\rangle$. The dipole moment is also used to determine the unit vector $\hat{\mathbf{e}}(t) = \delta\mathbf{M}(t)/\delta M(t)$ and the corresponding rotational correlation function

$$\Phi_r(t) = \langle \hat{\mathbf{e}}(t)\cdot\hat{\mathbf{e}}(0)\rangle \tag{17}$$

The relaxation time τ_r is the time integral of $\Phi_r(t)$.

The rotational relaxation time τ_r and the rotational diffusion constant $D_r = (2\tau_r)^{-1}$ are expected to be altered through the changing dipole moment of the solute affected by random torques of the medium. A linear scaling of τ_r with the squared protein dipole $\langle M\rangle^2$ predicted by classical theories of dielectric friction[3] (eq 2) is not supported by the present data (Figure S4 in SI). Predictions of standard theories of dielectric friction are thus violated for both the translational and rotational diffusion of proteins.

Figure 3 shows the temperature dependence of the diffusion coefficient for PC. The overall temperature law for this linear

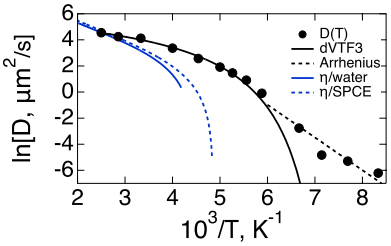

Figure 3. $\ln[D(T)]$ vs $1/T$ for PC. The solid line shows the fit to the VTF temperature law, $D(T) = D_0 \exp[-B/(T - T_0)]$ with $D_0 = 227$ μm^2/s, $B = 242$ K, and $T_0 = 130$ K. The dashed line shows the Arrhenius fit of three low-temperature points at $T = 120$, 130, 140, 150, and 170 K. Also shown are the experimental viscosity of bulk water[35] and of SPC/E water.[36] These two lines are shifted vertically to fit the scale of the plot.

transport coefficient is non-Arrhenius, similar to the diffusion constant for pure water and fragile glassforming materials.[37] A more careful analysis, however, reveals a fragile-to-strong crossover[38] of $D(T)$: the temperature dependence is non-Arrhenius at $T > T_{cross} \simeq 170$ K, followed with the Arrhenius temperature law at lower temperatures. Note that $T_g \simeq 170$ K is often identified with the glass transition of the protein hydration water,[15] which is somewhat higher that the glass transition temperature of bulk water, $\simeq$165 K[39,40] (previously identified at 136 K[41]). The solid line in Figure 3 is the fit to the Vogel–Tammann–Fulcher (VTF) temperature law $\ln[D] \propto B/(T - T_0)$. The fit results in the Kauzmann temperature[37] $T_0 \simeq 130$ K. It appears that the glass transition of the hydration shell intervenes before the anticipated divergence of the relaxation time. Also shown in Figure 3 are viscosities of bulk[35] and SPC/E[36] water (no $\eta(T)$ data for TIP3P water are available, to the best of our knowledge). It is clear that $\eta(T)$ does not match $D(T)$ for PC. This means that the Stokes–Einstein equation does not globally describe the protein diffusion constant,[42] and peculiarities seen in Figure 3 should be related to interfacial and not bulk water.

The compensation relation (eq 13) remains very accurate when considered as a function of the temperature. Figure 4a shows the results for the PC in TIP3P water (see SI for the simulation protocol). Equation 13 is satisfied in the entire range of simulated temperatures 100–400 K (red circles vs black crosses, Table S4 in SI). The total force variance scaled with β^2 shows a smooth variation with temperature (filled circles in Figure 4a). In contrast, the electrostatic component $\beta^2\langle(\delta\mathbf{F}_E)^2\rangle/3$ passes through a distinct maximum at $\simeq$200 K. The approach of the electrostatic force variance to the transition temperature from above is well described by the T^{-2} functionality.

The crossover at $T_{cross} \simeq 170$ K is reflected in the system dynamics. The relaxation time of the protein dipole $\tau_M(T)$, which is representative of the protein rotational dynamics, rises sharply on approach to T_{cross} (Figure 4b) and drops below this temperature, similarly to the variance of the electrostatic force in Figure 4a. The rotational relaxation time as predicted by hydrodynamics, $\tau_{0r} = 4\pi\beta\eta(T)R^3$ ($\tau_{0r} = (2D_{0r})^{-1}$ in eq 2), is compared to MD results in Figure 4b with $\eta(T)$ taken for SPC/E water.[36] The agreement is poor given differences between SPC/E's $\eta(T)$ used in the plot and TIP3P water used in the present simulations and potential distinctions in viscosities of interfacial and bulk water. Importantly, the non-Arrhenius character of $\eta(T)$ of bulk water does not account for high dynamical fragility[37] shown by $\tau_M(T)$.

The crossover temperature also marks a change in the non-Gaussian parameter[43,44] of the dipole moment (Figure 4c)

$$\chi = 1 - 3\langle(\delta\mathbf{M})^4\rangle/(5\langle(\delta\mathbf{M})^2\rangle^2) \tag{18}$$

One finds $\chi = 0$ for a freely rotating vector $\delta\mathbf{M}$ satisfying Gaussian statistics with a zero mean. A change in χ signals an alteration in the statistics of the protein dipole moment at the crossover temperature. Finally, we find that a strong separation between the component relaxation times $\tau_{E,LJ}$ and the total relaxation time τ_F (Table 1) exists only at high temperatures and all three times become close to each other at $T < T_{cross}$ (Figure 4d and Table S3 of SI). The crossover temperature T_{cross} thus marks a dramatic change in both the statistical and dynamical properties of protein hydration water.

To summarize, we report new results from MD simulations of diffusion of proteins in water, invalidating classical theories of dielectric friction, which predict a strong correlation of translational/rotational diffusion constants with the molecular multipole of the diffusing particle (eq 2). The failure of these theories is linked to the incorrect assumption of friction additivity for osmotic (vdW or LJ) and electrostatic forces acting on the protein from water. We instead find a remarkable insensitivity of the diffusion constant to the protein charge

https://doi.org/10.1021/acs.jpclett.4c02062
J. Phys. Chem. Lett. 2024, 15, 9502–9508

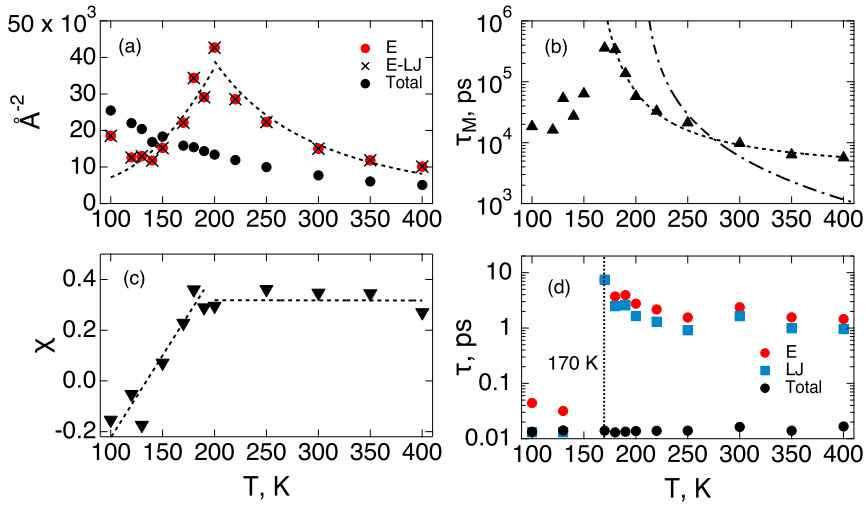

Figure 4. (a) Components of the force variance $\beta^2\langle(\delta\mathbf{F})^2\rangle/3$: E (red circles), negative of E−LJ (crosses, coinciding with the E component on the plot scale), and the total variance (black circles) vs T. The fit of the high-temperature data ($T \geq 200$ K) is with the $a + b/T^2$ function and the low-temperature data ($T < 200$ K) are fitted to a quadratic function (dashed lines). (b) Relaxation time $\tau_M(T)$ (black triangles) of the dipole moment (eq 16). The dashed line shows the VTF fit with $\tau_0 = 2750$ ps, $B = -193$ K, and $T_0 = 140$ K. The dash-dotted line shows the hydrodynamic rotational time, $\tau_{0r} = 4\pi\beta\eta(T)R^3$, with $R(\mathrm{PC}) = 14.1$ Å and $\eta(T)$ for SPC/E water.[36] (c) The non-Gaussian parameter $\chi(T)$ (eq 18, black triangles). The dashed lines are linear fits to guide the eye. (d) Force relaxation times $\tau_a(T)$, a = E, LJ, Total. All simulation results refer to wild-type PC.

varied here in a significantly broader range than attempted before. In contrast to diffusion in dilute solutions, the asymmetry of GFP's diffusion constant in cytosol in respect to its charge sign has been related to ribosomal and RNA's negative charges.[45]

The invariance of the diffusion constant in water with respect to the protein charge is a combined effect of the charge invariance of both the force variance and the force relaxation time. The Kirkwood relation for the diffusion constant is found to yield the diffusion constant within a factor of $\simeq 2$ when applied to proteins. At the same time, the Stokes−Einstein equation for the diffusion constant does not predict its scaling with the protein radius and is inconsistent with the temperature dependence of the diffusion constant.

Both a strongly non-Arrhenius $D(T)$ and the strong-to-fragile crossover at the glass transition temperature $T_{\mathrm{cross}} \simeq 170$ K found here still require explanation. The standard view of the origin of such phenomena is in terms of collective dynamics, involving many liquid particles, in low-temperature and metastable liquids.[37,46,47] In contrast, this behavior is found here for the diffusion of a single protein. The protein diffusion constant is affected by interfacial hydration water, which is mostly broken in dipolar domains oriented by local electric fields[18] and frustrated through their incompatible orientations.[48] It is not clear why this mosaic interfacial structure should promote a non-Arrhenius $D(T)$, unless surface domains propagate into the bulk on approach to T_{cross}. On the other hand, many of the features of the low-temperature dynamics of liquids arise from an increasing impact of electrostatics at low temperatures.[7] We indeed find a strong increase of the temperature reduced electrostatic force variance $\beta^2\langle(\delta\mathbf{F}_{\mathrm{E}})^2\rangle$ on approach to T_{cross} and a substantial spike in the relaxation time of the protein dipole reminiscent of critical slowing down.[49]

Because of the compensation between the electrostatic and LJ forces required by mechanical equilibrium, a spike in the electrostatic variance is accompanied by a corresponding spike in the LJ variance (Figure S5 of SI) to allow a smooth variation of the total variance with temperature (Figure 4a). Despite singularities in the temperature dependence of statistics and dynamics of component forces, the overall force variance, the force relaxation time, and the diffusion constant do not show any nonuniform features. Glass arrest of protein diffusion occurs in our study by lowering temperature but can be achieved by altering the ATP concentration in bacterial cells.[50,51]

■ ASSOCIATED CONTENT

Supporting Information

Simulation protocols, additional data, and the analysis of time correlation functions from MD simulations. The Supporting Information is available free of charge at https://pubs.acs.org/doi/10.1021/acs.jpclett.4c02062.

(PDF)

Transparent Peer Review report available (PDF)

■ AUTHOR INFORMATION

Corresponding Author

Dmitry V. Matyushov − *School of Molecular Sciences and Department of Physics, Arizona State University, Tempe, Arizona 85287-1504, United States;* orcid.org/0000-0002-9352-764X; Email: dmitrym@asu.edu

Author

Setare Mostajabi Sarhangi − *Department of Physics, Arizona State University, Tempe, Arizona 85287-1504, United States*

Complete contact information is available at: https://pubs.acs.org/10.1021/acs.jpclett.4c02062

Notes

The authors declare no competing financial interest.

■ ACKNOWLEDGMENTS

This research was supported by the National Science Foundation (CHE-2154465). The supercomputer time was provided through Extreme Science and Engineering Discovery Environment (XSEDE) allocation MCB080071 and through ASU's Research Computing. We are grateful to Prof Michael Colvin for sharing with us structures of GFP mutants.

■ REFERENCES

(1) Einstein, A. *Investigations on the Theory of the Brownian Movement*; BN Publishing, 2011.
(2) Born, M. Volumen und hydratationswärme der ionen. *Z. Phys.* **1920**, *1*, 45−48.
(3) Nee, T. W.; Zwanzig, R. R. Theory of dielectric relaxation in polar liquids. *J. Chem. Phys.* **1970**, *52*, 6353−6363.
(4) Hubbard, J.; Onsager, L. Dielectric dispersion and dielectric friction in electrolyte solutions. I. *J. Chem. Phys.* **1977**, *67*, 4850−4857.
(5) Zwanzig, R.; Harrison, A. K. Modifications of the Stokes-Einstein formula. *J. Chem. Phys.* **1985**, *83*, 5861−5862.
(6) Wolynes, P. Dynamics of electrolyte solutions. *Annu. Rev. Phys. Chem.* **1980**, *31*, 345−376.
(7) Samanta, T.; Matyushov, D. V. Dielectric friction, violation of the Stokes-Einstein-Debye relation, and non-Gaussian transport dynamics of dipolar solutes in water. *Phys. Rev. Res.* **2021**, *3*, 023025.
(8) Matyushov, D. V. War and peace between electrostatic and van der Waals forces regulate translational and rotational diffusion. *J. Chem. Phys.* **2022**, *157*, 080901.
(9) Sarhangi, S. M.; Matyushov, D. V. Driving forces of protein diffusivity. *J. Phys. Chem. Lett.* **2020**, *11*, 10137−10143.
(10) Lawrence, M. S.; Phillips, K. J.; Liu, D. R. Supercharging proteins can impart unusual resilience. *J. Am. Chem. Soc.* **2007**, *129*, 10110−10112.
(11) Lau, E. Y.; Phillips, J. L.; Colvin, M. E. Molecular dynamics simulations of highly charged green fluorescent proteins. *Mol. Phys.* **2009**, *107*, 1233−1241.
(12) Drobizhev, M.; Callis, P. R.; Nifosì, R.; Wicks, G.; Stoltzfus, C.; Barnett, L.; Hughes, T. E.; Sullivan, P.; Rebane, A. Long- and Short-Range Electrostatic Fields in GFP Mutants: Implications for Spectral Tuning. *Sci. Rep.* **2015**, *5*, 13223.
(13) Lin, C.-Y.; Romei, M. G.; Oltrogge, L. M.; Mathews, I. I.; Boxer, S. G. Unified model for photophysical and electro-optical properties of green fluorescent proteins. *J. Am. Chem. Soc.* **2019**, *141*, 15250−15265.
(14) Jorgensen, W. L.; Chandrasekhar, J.; Madura, J. D.; Impey, R. W.; Klein, M. L. Comparison of simple potential functions for simulating liquid water. *J. Chem. Phys.* **1983**, *79*, 926−935.
(15) Doster, W.; Busch, S.; Gaspar, A. M.; Appavou, M.-S.; Wuttke, J.; Scheer, H. Dynamical transition of protein-hydration water. *Phys. Rev. Lett.* **2010**, *104*, 098101.
(16) Doster, W. The two-step scenario of the protein dynamical transition. *J. Non-Cryst. Solids* **2011**, *357*, 622−628.
(17) Khodadadi, S.; Sokolov, A. P. Protein dynamics: from rattling in a cage to structural relaxation. *Soft Matter* **2015**, *11*, 4984−4998.
(18) Martin, D. R.; Matyushov, D. V. Dipolar nanodomains in protein hydration shells. *J. Phys. Chem. Lett.* **2015**, *6*, 407−412.
(19) Hummer, G.; Pratt, L. R.; García, A. E. Ion sizes and finite-size corrections for ionic-solvation free energies. *J. Chem. Phys.* **1997**, *107*, 9275−9277.
(20) Ito, K.; Moynihan, C. T.; Angell, C. A. Thermodynamic determination of fragility in liquids and a fragile-to-strong liquid transition in water. *Nature* **1999**, *398*, 492.
(21) Hansen, J.-P.; McDonald, I. R. *Theory of Simple Liquids*, 4th ed.; Academic Press: Amsterdam, 2013.
(22) Balucani, U.; Zoppi, M. *Dynamics of the Liquid Phase*; Clarendon Press: Oxford, 1994.
(23) Mori, H. Transport, collective motion, and Brownian motion. *Prog. Theor. Phys.* **1965**, *33*, 423−455.
(24) Shin, H. K.; Kim, C.; Talkner, P.; Lee, E. K. Brownian motion from molecular dynamics. *Chem. Phys.* **2010**, *375*, 316−326.
(25) Yeh, I. C.; Hummer, G. System-size dependence of diffusion coefficients and viscosities from molecular dynamics simulations with periodic boundary conditions. *J. Phys. Chem. B* **2004**, *108*, 15873−15879.
(26) Hafner, R.; Guevara-Carrion, G.; Vrabec, J.; Klein, P. Sampling the bulk viscosity of water with molecular dynamics simulation in the canonical ensemble. *J. Phys. Chem. B* **2022**, *126*, 10172−10184.
(27) Terry, B. R.; Matthews, E. K.; Haseloff, J. Molecular characterization of recombinant green fluorescent protein by fluorescence correlation microscopy. *Biochem. Biophys. Res. Commun.* **1995**, *217*, 21−27.
(28) Guiot, E.; Enescu, M.; Arrio, B.; Johannin, G.; Roger, G.; Tosti, S.; Tfibel, F.; Mérola, F.; Brun, A.; Georges, P.; et al. Molecular dynamics of biological probes by fluorescence correlation microscopy with two-photon excitation. *J. Fluoresc.* **2000**, *10*, 413−419.
(29) Mika, J. T.; Schavemaker, P. E.; Krasnikov, V.; Poolman, B. Impact of osmotic stress on protein diffusion in Lactococcus lactis. *Mol. Microbiol.* **2014**, *94*, 857−870.
(30) Wang, Z.; Shah, J. V.; Chen, Z.; Sun, C.-H.; Berns, M. W. Fluorescence correlation spectroscopy investigation of a GFP mutant-enhanced cyan fluorescent protein and its tubulin fusion in living cells with two-photon excitation. *J. Biomed. Optics* **2004**, *9*, 395−403.
(31) Mika, J. T.; Poolman, B. Macromolecule diffusion and confinement in prokaryotic cells. *Curr. Opin Biotechnol* **2011**, *22*, 117−126.
(32) Sarhangi, S. M.; Matyushov, D. V. Effect of water deuteration on protein electron transfer. *J. Phys. Chem. Lett.* **2023**, *14*, 723−729.
(33) Cui, A. Y.; Cui, Q. Modulation of nanoparticle diffusion by surface ligand length and charge: Analysis with molecular dynamics simulations. *J. Phys. Chem. B* **2021**, *125*, 4555−4565.
(34) Mukherjee, K.; Palchowdhury, S.; Maroncelli, M. Do electrostatics control the diffusive dynamics of solitary water? NMR and MD studies of water translation and rotation in dipolar and ionic solvents. *J. Phys. Chem. B* **2024**, *128*, 3689−3706.
(35) Dehaoui, A.; Issenmann, B.; Caupin, F. Viscosity of deeply supercooled water and its coupling to molecular diffusion. *Proc. Natl. Acad. Sci. U.S.A.* **2015**, *112*, 12020−12025.
(36) Meyer, N.; Piquet, V.; Wax, J. F.; Xu, H.; Millot, C. Rotational and translational dynamics of the SPC/E water model. *J. Mol. Liq.* **2019**, *275*, 895−908.
(37) Angell, C. A. Formation of glasses from liquids and biopolymers. *Science* **1995**, *267*, 1924−1935.
(38) Angell, C. A.; Ngai, K. L.; McKenna, G. B.; McMillan, P. F.; Martin, S. W. Relaxation in glassforming liquids and amorphous solids. *J. Appl. Phys.* **2000**, *88*, 3113.
(39) Yue, Y.; Angell, C. A. Clarifying the glass-transition behaviour of water by comparison with hyperquenched inorganic glasses. *Nature* **2004**, *427*, 717−720.
(40) Giovambattista, N.; Angell, C. A.; Sciortino, F.; Stanley, H. E. Glass-transition temperature of water: A simulation study. *Phys. Rev. Lett.* **2004**, *93*, 047801.
(41) Johari, G. P.; Hallbrucker, A.; Mayer, E. The glass−liquid transition of hyperquenched water. *Nature* **1987**, *330*, 552−553.
(42) Sadoon, A. A.; Oliver, W. F.; Wang, Y. Revisiting the temperature dependence of protein diffusion inside bacteria: Validity of the Stokes-Einstein equation. *Phys. Rev. Lett.* **2022**, *129*, 018101.
(43) Rahman, A. Correlations in the motion of atoms in liquid argon. *Phys. Rev.* **1964**, *136*, A405−A411.
(44) Sauer, M.; Colburn, T.; Maiti, S.; Heyden, M.; Matyushov, D. V. Linear and nonlinear dielectric response of intrinsically disordered proteins. *J. Phys. Chem. Lett.* **2024**, *15*, 5420−5427.
(45) Schavemaker, P. E.; Śmigiel, W. M.; Poolman, B. Ribosome surface properties may impose limits on the nature of the cytoplasmic proteome. *eLife* **2017**, *6*, No. e30084.
(46) Stillinger, F. H.; Debenedetti, P. G. Glass transition thermodynamics and kinetics. *Annu. Rev. Condens. Matter Phys.* **2013**, *4*, 263−285.

https://doi.org/10.1021/acs.jpclett.4c02062
J. Phys. Chem. Lett. 2024, 15, 9502−9508

(47) Debenedetti, P. G. *Metastable Liquids: Concepts and Principles*; Princeton University Press: Princeton, NJ, 1996.
(48) Martin, D. R.; Forsmo, J. E.; Matyushov, D. V. Complex dynamics of water in protein confinement. *J. Phys. Chem. B* **2018**, *122*, 3418−3425.
(49) Stanley, H. E. *Introduction to Phase Transitions and Critical Phenomena*; Oxford University Press: New York, 1987.
(50) Parry, B. R.; Surovtsev, I. V.; Cabeen, M. T.; O'Hern, C. S.; Dufresne, E. R.; Jacobs-Wagner, C. The bacterial cytoplasm has glass-like properties and is fluidized by metabolic activity. *Cell* **2014**, *156*, 183−194.
(51) Åberg, C.; Poolman, B. Glass-like characteristics of intracellular motion in human cells. *Biophys. J.* **2021**, *120*, 2355−2366.

https://doi.org/10.1021/acs.jpclett.4c02062
J. Phys. Chem. Lett. 2024, 15, 9502−9508